ISSN 1330–0016
CODEN FIZBE7

# ELECTROMAGNETIC FEW–BODY RESPONSE FUNCTIONS WITH THE LORENTZ INTEGRAL TRANSFORM

WINFRIED LEIDEMANN[a], VICTOR D. EFROS[b], GIUSEPPINA ORLANDINI[a], and EDWARD L. TOMUSIAK[c]

[a] *Dipartimento di Fisica, Università di Trento, I-38050 Povo, Italy and Istituto Nazionale di Fisica Nucleare, Gruppo collegato di Trento*

[b] *Russian Research Centre "Kurchatov Institute", Kurchatov Square 1, 123182 Moscow, Russia*

[c] *Department of Physics and Engineering Physics and Saskatchewan Accelerator Laboratory, University of Saskatchewan, Saskatoon, Canada S7N 0W0*

Received 15 January 1999; Accepted 12 July 1999

The Lorentz integral transform method is described briefly. The resulting differential equations are solved via an expansion in hypersherical harmonics, and a new approach is introduced for incorporating correlations in the basis functions. New results for the total photoabsorption cross section of $^3$H and $^3$He are presented. It is shown that the peak of the cross section is strongly affected by the three-nucleon force. In addition, we review the results for the $^4$He electromagnetic response functions obtained with the Lorentz integral transform method.

PACS numbers: 21.45.+v, 25.20.-x UDC 539.128, 539.171

Keywords: Lorentz integral transform, hypersherical harmonics, total photoabsorption cross section, $^3$H and $^3$He, three-nucleon force, $^4$He electromagnetic response functions

## 1. *Introduction*

The Lorentz integral transform method [1] is a novel method for treating exactly final-state interactions in inclusive few–body response functions. It makes the explicit calculation of the final-state wave function unnecessary. Therefore, the numerical effort is reduced drastically compared to the usual way of calculation. So far the method has been applied to the calculation of the longitudinal (e,e') responses of three– and four-nucleon systems [2–4] and to their total photoabsorption cross sections [5–7]. While all the $^4$He responses were calculated with semirealistic

central potentials, realistic interactions have also been used in Refs. 2 and 7 for the responses of the three–nucleon system. In the case of the total photoabsorption cross section [7], however, the only realistic NN interaction which has been used is the super soft core TRSB potential [8]. First results with other realistic potential models will be presented in this paper, where we consider the AV14 potential [9] and the UrbanaVIII three–nucleon force (URBVIII 3N–force) [10]. The strong and rather state-dependent short-range repulsion requires the inclusion of state-dependent NN correlations in our basis functions. The next section describes a new procedure we use for the inclusion of these correlations.

First, we will briefly describe the method of the Lorentz integral transform. The inclusive response function of a system to an external probe has the form

$$R(\omega) = \int \mathrm{d}f |\langle \Psi_f | \hat{O} | \Psi_0 \rangle|^2 \delta(E_f - E_0 - \omega) \,, \tag{1}$$

where $\hat{O}$ is a transition operator which characterizes the process under consideration, $\Psi_0$ and $\Psi_f$ are the ground-state wave function and a complete set of final-state wave functions, respectively, while $\omega$ denotes the excitation energy. The Lorentz transform of $R$ is given by

$$\Phi(\sigma_R, \sigma_I) = \int\limits_{\omega_{\min}}^{\infty} \mathrm{d}\omega \frac{R(\omega)}{(\omega - \sigma_R)^2 + \sigma_I^2} \,. \tag{2}$$

Due to the resonant shape of the kernel, even complicated structures in $R$ can be resolved if a sufficiently small $\sigma_I$ is chosen.

The method proceeds in two steps. First, the left–hand side of Eq. (2) is calculated. This is accomplished with the help of closure

$$\begin{aligned} \Phi(\sigma_R, \sigma_I) &= \langle \Psi_0 | \, \hat{O}^\dagger (H - E_0 - \sigma_R - \mathrm{i}\sigma_I)^{-1} (H - E_0 - \sigma_R + \mathrm{i}\sigma_I)^{-1} \hat{O} \, | \Psi_0 \rangle \\ &= \langle \tilde{\Psi} | \tilde{\Psi} \rangle \,, \end{aligned} \tag{3}$$

where $E_0$ is the ground-state energy of the Hamiltonian $H$, and $\tilde{\Psi}$ is determined by the equation

$$(H - E_0 - \sigma_R + \mathrm{i}\sigma_I) | \tilde{\Psi} \rangle = \hat{O} | \Psi_0 \rangle \,. \tag{4}$$

Because of Eq. (3), the norm of $\tilde{\Psi}$ exists and thus, contrary to continuum wave functions, $\tilde{\Psi}$ vanishes at large distances like a bound state wave function. Therefore, the solution of Eq. (4) is much simpler than that of the continuum state Schrödinger equation.

The second step is the inversion of the transform $\Phi$ in order to obtain $R(\omega)$. For this purpose, $\Phi$ is calculated for a set of positive $\sigma_R$ values with a fixed $\sigma_I > 0$. Details of the inversion are discussed in Ref. 7.

## 2. Formalism

We solve Eq. (3) and the Schrödinger equation for the nuclear ground-state wave function as an expansion over a set of basis functions. Eventually, it leads to a system of linear equations for the expansion coefficients. The basis functions $\phi_i$ are antisymmetric with respect to particle permutation. They consist of products of a spin–isospin part $\theta_\mu$ and a spatial part $\chi_{i,\tilde{\mu}}$. Both parts have a given type of permutational symmetry in order to guarantee a totally antisymmetric wave function. For the spatial part, we use products of symmetrized hyperspherical harmonics (HH) and hyperradial functions. The HH expansion is made to a maximal value of $K$, where $K$ is the generalized angular momentum quantum number. Further details of the basis functions as well as the technique for the calculation of the matrix element of the Hamiltonian are described in Ref. 7.

In our previous calculations, we applied state-independent correlation functions, i.e. a multiplication of the basis functions by a Jastrow correlation factor $\prod_{i<j} f(r_{ij})$. In the present work, we use spin-isospin dependent correlation functions $f_{ST}(r)$. To this end, we define a state-dependent Jastrow correlation operator

$$\hat{\omega} = \hat{S}[\prod_{i<j} \sum_{ST} f_{ST}(r_{ij}) \hat{P}_{ST}(ij)] \tag{5}$$

with

$$\hat{P}_{ST}(ij) = \frac{1 \pm (ij)_S}{2} \, \frac{1 \pm (ij)_T}{2} \, . \tag{6}$$

Here $\hat{P}_{ST}$ are the projection operators onto a given spin and isospin state of a nucleon pair, $(ij)_{S,T}$ are permutation operators of spin and isospin of particles $i$ and $j$, $f_{ST}$ are the pair-correlation functions depending on the interparticle distance $r_{ij}$, $\hat{S}$ is the symmetrizer with respect to the ordering of particle pairs [10,11]. We do not include tensor correlations in Eq. (5) since normally only central components of the potential lead to strong short-range repulsion. Correlations of longer range are presumably sufficiently described directly by our basis functions without making it necessary to include HH functions with a very high $K$.

In the three–body case, which is considered in this work, the correlation operator is presented by the matrix

$$\omega_{\lambda\mu} = \sum_{i1,i2,i3=1}^{4} f_{i_1}(r_{12}) f_{i_2}(r_{13}) f_{i_3}(r_{23}) M(\lambda, \mu; i1, i2, i3) \tag{7}$$

with

$$M(\lambda, \mu; i1, i2, i3) = \langle \theta_\lambda | \hat{S} (\hat{P}_{i_1}(12) \hat{P}_{i_2}(13) \hat{P}_{i_3}(23) | \theta_\mu \rangle \, . \tag{8}$$

Once the matrix $M(\lambda, \mu; i1, i2, i3)$ is calculated, the new basis functions are defined

by

$$\phi_i^{new} = \sum_{\lambda,\mu} [\omega_{\lambda,\mu} \chi_{i,\tilde{\mu}} \theta_\lambda] \,. \tag{9}$$

The calculation then proceeds in the same way as for an uncorrelated basis.

We would like to point out that the above method of introducing correlations incorporates correlations after symmetrization of the wave function. This is different from the approach of Ref. 12, where the correlation is inserted before symmetrization. As opposed to our method, this does not guarantee that an NN pair with a specific $ST$ value is always correlated with the corresponding $ST$ correlation function.

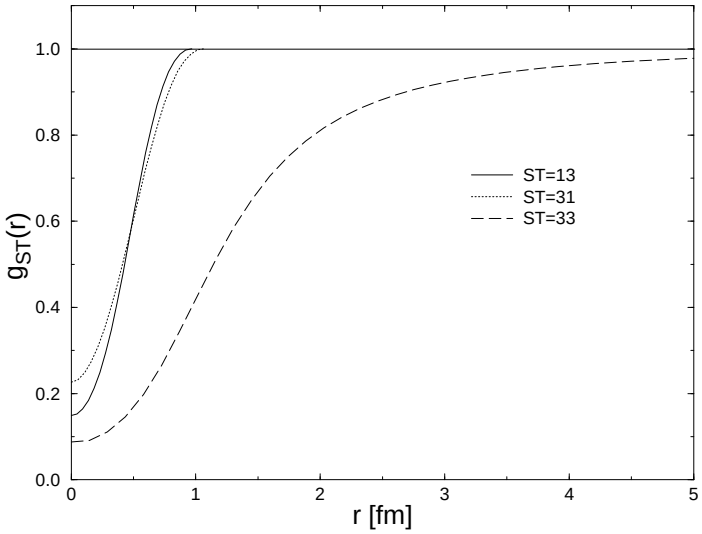


*Fig. 1. The correlation functions $g_{ST}(r)$ for $ST$ = 13, 31 and 33.*

The correlation functions $f_{ST}(r)$ are obtained as follows. For any NN potential, we take them at $r < r_0$ as the zero-energy pair wave functions in the corresponding $ST$-state. The distance $r_0$ represents the healing distance. This implies that $f(r) = 1$ at $r > r_0$ and $f'(r_0) = 0$. The $ST$ pair wave functions are calculated in the following way. For $ST = 11, 13, 31$ and 33, we take the potential for the NN partial waves $^1\mathrm{P}_1$,$^1\mathrm{S}_0$,$^3\mathrm{S}_1$ and $^3\mathrm{P}_1$, respectively. For $ST$ =11 and 33, however, the potentials are not sufficiently attractive in order to obtain a healing distance. Therefore, we introduce an additional central attraction of intermediate range. The strength of the additional interaction is fitted such that a healing distance of 10 fm is obtained.

The presence of other nucleons in a nucleus alters the free correlations of a nucleon pair. We try to incorporate such effects by the introduction of a scaling factor $\alpha_{ST}$ for the argument of the correlation function, i.e. instead of $f_{ST}(r)$ we take a new correlation function $g_{ST}(r) = f_{ST}(\alpha_{ST}\, r)$. The scaling factors are fitted

in order to obtain the highest possible binding energy for the ground state, taking an expansion of the ground-state wave function up to $K = 10$. The fits lead to modified healing distances of $r_0/\alpha$. For $ST = 13$, 31, we find $\alpha$–values rather close to 1, while there are larger effects for the other two channels ($\alpha_{33} \simeq 1.45$, $\alpha_{11} \simeq 0.5$). The correlation functions found for the bound state are used in solving Eq. (4) without changes. The correlation functions for $ST = 13$, 31, and 33 are illustrated in Fig.1.

## 3. Results and discussion

First, we discuss the total photoabsorption cross section of the three–nucleon systems. It is well known that the cross section is reliably calculated in dipole approximation. In this case, one has to consider the response function

$$R(E_\gamma) = \int \mathrm{d}f |\langle f|D_z|0\rangle|^2 \delta(E_f - E_0 - E_\gamma)\,, \tag{10}$$

where $D_z$ is the nuclear dipole operator. The cross section is given by

$$\sigma_T = 4\pi^2 (e^2/\hbar c) E_\gamma R(E_\gamma). \tag{11}$$

Formerly, we calculated $\sigma_T$ employing semirealistic potential models [6] and the realistic TRSB NN interaction [7]. Here we also consider the AV14 NN potential and the URBVIII 3-N force. First, we briefly discuss our results for the ground state. The correlation operator we use allows a reduction of the number of the basis functions to be retained in the calculation. For a further reduction, we select subsystems of HH from their complete sets at given high $K$ values. We find that it is sufficient to include only basis functions, where the relative pair and third-particle angular momentum quantum numbers before the symmetrization are less or equal 2, and we checked that other basis functions contribute only negligibly to the three-nucleon binding energy. In the early work, starting from Ref. 13, such a selection has been used with no correlation operator applied to the basis functions, and we thus find that the selection is effective also in conjunction with the Jastrow correlations.

With a maximal $K$ value of 34, we have a sufficiently good convergence of the HH expansion for the binding energy, we obtain 7.64 MeV (AV14) and 8.47 MeV (AV14+URBVIII). From an extrapolation of $K$ to infinity via a Pade approximation, we estimate a missing binding energy of less than 0.05 MeV. The binding energies for both potential models agree well with the values in the literature (7.67 MeV [14], 8.46 MeV [10,14]).

For $\tilde{\Psi}$ of Eq. (4), whose norm gives the Lorentz integral transform, we make an expansion up to a maximal $K$ of 15. As in Ref. 7 for the TRSB potential, we find that the Lorentzian transform for the isospin channel $T = 3/2$ has a very rapid convergence. However, for the $T = 1/2$ channel, we have a much slower convergence than for the TRSB potential. In principle, higher values of $K$ are needed in order

to have a satisfactory convergence. In the future, we will improve our results by extending the calculation to higher $K$. This is not trivial, however, since the number of

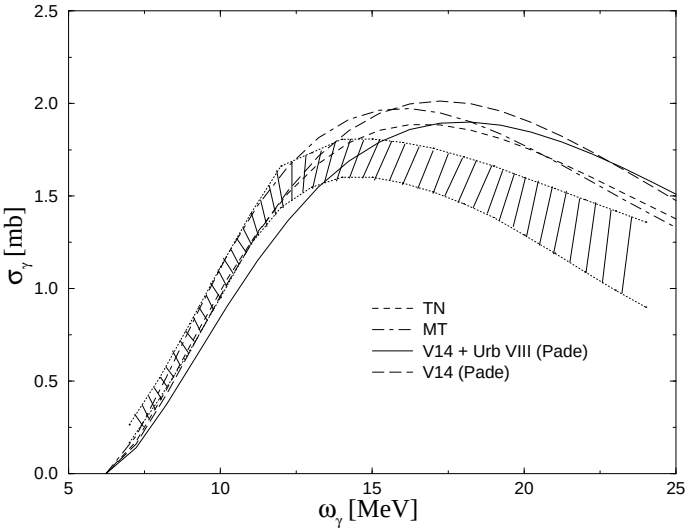


*Fig. 2. Triton total photoabsorption cross section with AV14 potential (long dashed curve) and AV14 plus URBVIII* 3N*–force (full curve) in Pade approximation (see text), also shown results with MT (dash-dotted curve) and TN potential (short dashed curve); experimental data from Ref. [17] (represented by the error band).*

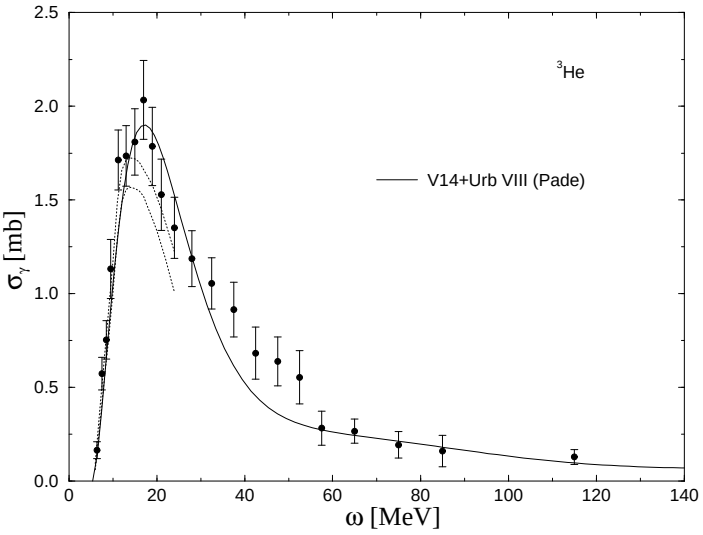


*Fig. 3.* $^3$He *total photoabsorption cross section with AV14 potential plus URBVIII* 3N*–force (full curve) in Pade approximation (see text); experimental data from Refs. [17] (error band is represented by the dotted curves) and [18] (full circles).*

basis states is already rather large and we cannot simply increase $K$ to much larger values. Therefore, we have to study whether some of the HH basis states do not contribute and can simply be omitted. Here, we will show results, where the $T = 1/2$ part of the transform is calculated with the help of a Pade approximation. As input, we take the $T = 1/2$ transforms with a maximal $K$ of 11, 13, and 15. The additional contribution to the transform due to the Pade approximation is at most of the order of 5%. The correction is not very sizeable, but nevertheless our results have to be considered preliminary. The calculated effect of the 3N–force should be rather reliable, since we do not think that the missing contribution of the higher $K$ values is sensitive to the 3N–force.

In Fig. 2, we show the total photoabsorption cross section of $^3$H for various potential models in the low–energy region. It is evident that the 3N–force leads to a rather strong reduction of the peak height. However, one has to consider that the correct description of the nuclear bound state is rather important for the low-energy cross section. This can already be understood form the inverse energy weighted sum rule, which is proportional to the square of the proton point radius of $^3$H. A simple scaling of the cross section with the square of these radii for AV14 and AV14+URBVIII would lead to a reduction of the AV14 cross section by 7.7 %.

Compared to the available experimental cross sections shown in Fig. 2, one finds a rather good but not totally satisfactory agreement. To make a final conclusion, we must await our improved calculation with higher $K$ for the $T = 1/2$ transform. In Fig. 2, we also illustrate results with two semirealistic central potentials (MT

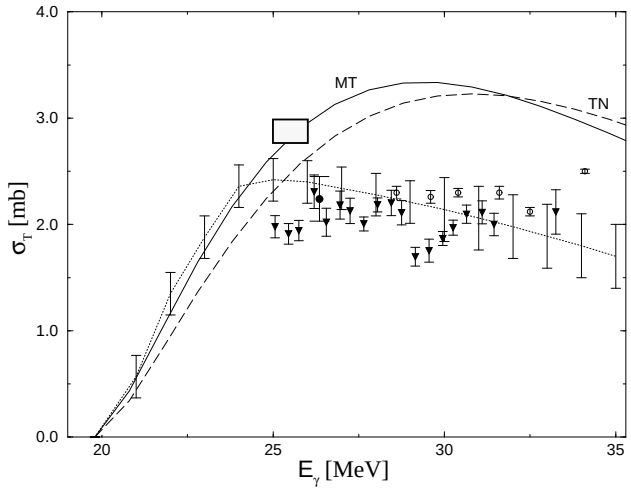


*Fig. 4. Total* $^4$He *photoabsorption cross section with MT and TN potentials. Experimental cross sections: shaded area [19]; sum of partial cross section for total neutron breakup [20] and two–body proton breakup [21] (dotted curve with typical size of the experimental error). Also shown are doubled experimental cross sections for two–body proton breakup [22] (open circles) and for two–body neutron breakup [23] (triangles) and [24] (full circles) (for further explanation see text).*

potential [16], TN potential [7]). It is interesting to see that they lead to results rather similar to the more realistic interactions.

In Fig. 3, we show the $^3$He cross section in an extended energy range compared to the experimental data. One sees a rather good agreement with experimental data over the whole energy range.

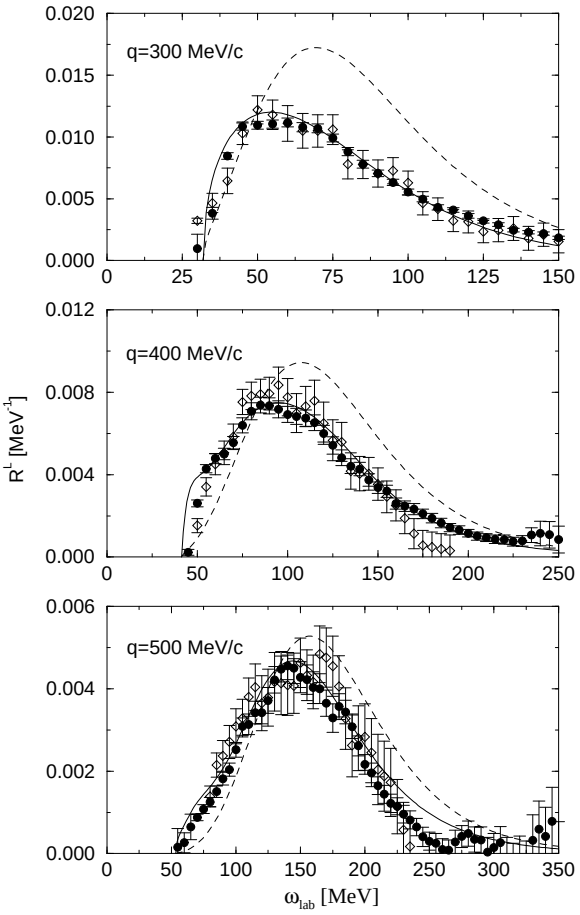


*Fig. 5. Longitudinal response functions of* $^4$He *with TN potential (full curves) in comparison to the experimental data of Refs. [26] (diamonds) and [27] (full circles). The quasielastic response is also shown (dashed curve).*

Next, we turn to the $^4$He total photodisintegration cross section. In Fig. 4, we show our figure from Ref. 5 but including here also a total photoabsorption cross section which is determined from elastic photon scattering [19]. Only this data point and the dotted curve of Fig. 4 (sum of cross sections of all neutron breakup channels plus cross section of p$^3$H channel) can be considered as direct experimental data for the total cross section. All other cases are pseudo data, where we have simply doubled the cross sections for the two–body breakup cross sections (n$^3$He, p$^3$H)

assuming that these two channels are more or less equal and dominant for the low–energy cross section. It is readily evident that a much more pronounced peak of the giant dipole resonance is predicted with the semirealistic potential models. Only the experimental point extracted from photon scattering comes closer to the theoretical cross sections. Considering the triton results of Fig. 2, one would not expect that the semirealistic potential models would give such an overly large cross section for $^4$He. Moreover, the integrated cross section (TRK sum rule) has been evaluated with realistic potential models [16], and these values are considerably larger than the TRK sum rule value with MT and TN potentials.

Next, we consider the longitudional (e,e') response function of $^4$He. As transition operator, we take the one–body charge operator

$$Q = \frac{1}{2}\sum_{k=1}^{A}(G_E^p[1+\tau_{z,k}] + G_E^n[1-\tau_{z,k}])\exp[i\mathbf{q}\cdot(\mathbf{r_k}-\mathbf{R_{cm}})]\,. \qquad (12)$$

Here $G_E^p$ and $G_E^n$ are the modified [25] free proton and neutron electric form factors, respectively, while $\tau_{z,k}$ denotes the third component of the isospin of the $k$th nucleon.

In Fig. 5, we show the longitudinal response function $^4$He for the momentum transfers $q = 300$, 400 and 500 MeV/$c$ from Refs. 3 and 4 calculated with the semirealistic TN potential. For all three-momentum transfers, one sees a good agreement between theory and experiment. Figure 5 also contains the results of a plane-wave

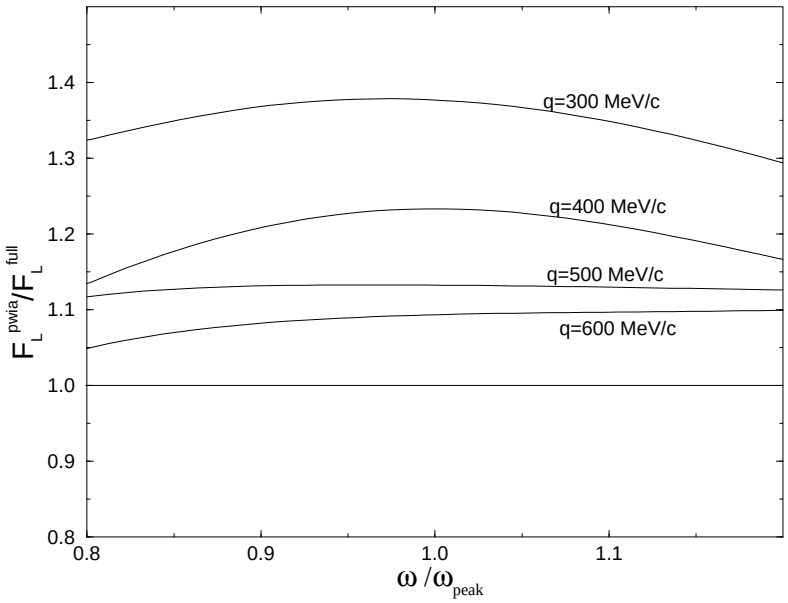


*Fig. 6. Ratios of quasifree and full* $^4$He *longitudinal response functions for various momentum transfers.*

impulse approximation (PWIA), which has been calculated using the exact spectral function of $^4$He for the TN potential [4]. At $q = 300$ MeV/$c$, one finds rather large differences, but for the higher momentum transfers, the peak region is described much better. In Fig. 6, we show the ratio of the PWIA and exact responses, where also $q = 600$ MeV/$c$ is included [7]. The comparison shows that the PWIA response is a rather good approximation in the peak region. The quality of the approximation improves with increasing momentum transfer, indicating an error of only a few percent for $q$ greater than 1 GeV/$c$.

## *4. Summary*

We have shown that the Lorentz integral transform approach is a very fruitful method. It leads to a drastic reduction in the numerical calculation for few–body response functions. This enabled us to make various realistic calculations for the first time (e.g. three– and four–body total photoabsorption cross sections, $^4$He spectral function). In this work, we have introduced a new correlation scheme for few–nucleon calculations. Furthermore, we could show that there are rather strong effects of the 3N–force on the low–energy peak in the three–nucleon photodisintegration. However, as mentioned, we still have to improve our calculation in order to obtain a completely convergent HH expansion for the Lorentz integral transform. It will be very interesting to have the complete results with and without the effects of the 3N–force.

References


1) V. D. Efros, W. Leidemann and G. Orlandini, Phys. Lett. B **338** (1994) 130;
2) S. Martinelli, H. Kamada, G. Orlandini and W. Glöckle, Phys. Rev. C **52** (1995) 1778;
3) V. D. Efros, W. Leidemann and G. Orlandini, Phys. Rev. Lett. **78** (1997) 432;
4) V. D. Efros, W. Leidemann and G. Orlandini, Phys. Rev. C **58** (1998) 582;
5) V. D. Efros, W. Leidemann and G. Orlandini, Phys. Rev. Lett. **78** (1997) 4015;
6) V. D. Efros, W. Leidemann and G. Orlandini, Phys. Lett. B **408** (1997) 1;
7) V. D. Efros, W. Leidemann and G. Orlandini, Few-Body Syst. **26** (1999) 251;
8) R. De Tourreil, B. Rouben and D. W. L. Sprung, Nucl. Phys. A **242** (1975) 465; J. Côte, R. De Tourreil, B. Rouben and D. W. L. Sprung, Nucl. Phys. A **A273** (1976) 269;
9) R. B. Wiringa, R. A. Smith and T. L. Ainsworth, Phys. Rev. C **29** (1984) 1207;
10) R. B. Wiringa, Phys. Rev. C **43** (1991) 1585;
11) V. R. Pandharipande and R. B. Wiringa, Nucl. Phys. A **266** (1976) 269;
12) A. Kievsky, M. Viviani and S. Rosati, Nucl. Phys. A **551** (1993) 241;
13) V. D. Éfros, Sov. J. Nucl. Phys. **15**, 128 (1972); V. F. Demin, Yu. E. Pokrovsky and V. D. Efros, Phys. Lett. B **44** 227 (1973);
14) C. R. Chen, G. L. Payne, J. L. Friar and B. F. Gibson, Phys. Rev. C **31** (1985) 2266;

15) R. A. Malfliet and J. Tjon, Nucl. Phys. A **127** (1969) 161;

16) W. Heinze, H. Arenhövel and G. Horlacher, Phys. Lett. B **76** (1978) 379; M. Gari, H. Hebach, B. Sommer and J. G. Zabolitzky, Phys. Rev. Lett. **41** (1978) 1288; R. Schiavilla, A. Fabrocini and V. R. Pandharipande, Nucl. Phys. A **473** (1987) 290;

17) D. D. Faul, B. L. Berman, P. Meyer and D. Olson, Phys. Rev. C **24** (1981) 849, and references therein;

18) V. N. Fetisov, A. N. Gorbunov and A. T. Varfolomeev, Nucl. Phys. A **71** (1965) 305;

19) D. P. Wells, D. S. Dale, R. A. Eisenstein, F. J. Federspiel, M. A. Lucas, K. E. Mellendorf, A. M. Nathan and A. E. O'Neill, Phys. Rev. C **46** (1992) 449;

20) B. L. Berman, D. D. Faul, P. Meyer and D. L. Olson, Phys. Rev. C **22** (1980) 2273;

21) G. Feldman, M. J. Balbes, L. H. Kramer, J. Z. Williams, H. R. Weller and D. R. Tilly, Phys. Rev. C **42** (1990) 1167;

22) R. Bernabei et al., Phys. Rev. C **38** (1988) 1990;

23) L. Ward, D. R. Tilly, D. M. Skopik, N. R. Robertson and H. R. Weller, Phys. Rev. C **24** (1981) 317;

24) J. Asai, G. Feldman, R. E. J. Florizone, E. L. Hallin, D. M. Skopik, J. M. Vogt, R. C. Haight and S. M. Sterbenz, Few-Body Syst. Suppl. **7** (1994) 136;

25) J. L. Friar, Ann. Phys. **81** (1973) 332; T. De Forest, Jr., Nucl. Phys. A **414** (1984) 347;

26) S. A. Dytman, A. M. Bernstein, K. I. Blomqvist, T. J. Pavel, B. P. Quinn, R. Altemus, J. S. McCarthy, G. H. Mechtel, T. S. Ueng and R. R. Whitney, Phys. Rev C **38** (1988) 800;

27) A. Zghiche, Nucl. Phys. A **572** (1994) 513.

## ELECTROMAGNETSKE ODZIVNE FUNKCIJE ZA NEKOLIKO TIJELA I LORENTZOVA INTEGRALNA TRANSFORMACIJA

Kratko se opisuje metoda Lorentzove integralne transformacije. Dobiju se diferencijalne jednadžbe koje se rješavaju razvojem po hipersferičnim harmonicima i uvodi se nov pristup radi uključivanja korelacija među osnovnim funkcijama. Prikazuju se novi ishodi računa za ukupni udarni presjek fotoapsorpcije $^3$H i $^3$He. Pokazuje se kako na vrh udarnog presjeka jako utječu tro-nukleonske sile. Još se daje pregled ishoda računa za elektromagnetske odzivne funkcije $^4$He koji su postignuti metodom Lorentzove integralne transformacije.